Journal of Applied Pharmaceutical Science Vol. 13(07), pp 270-281, July, 2023
Available online at http://www.japsonline.com
DOI: 10.7324/JAPS.2023.117321
ISSN 2231-3354

# Antitrypanosomal potential of the red sea soft coral *Nephthea mollis* supported by metabolomics profiling and molecular docking studies

Khaled M. Allam[1*], Yaser A. Mostafa[2], Usama R. Abdelmohsen[3,6], Amgad I.M. Khedr[4], Ahmed E. Allam[5], Ehab S. Elkhayat[5], Mostafa A. Fouad[6]

[1]Department of Pharmacognosy, Faculty of Pharmacy, South Valley University, Qena, Egypt.
[2]Pharmaceutical Organic Chemistry Department, Faculty of Pharmacy, Assiut University, Assiut, Egypt.
[3]Department of Pharmacognosy, Faculty of Pharmacy, Deraya University, Minia, Egypt.
[4]Department of Pharmacognosy, Faculty of Pharmacy, Port Said University, Port Said, Egypt.
[5]Department of Pharmacognosy, Faculty of Pharmacy, Al-Azhar University, Assiut, Egypt.
[6]Department of Pharmacognosy, Faculty of Pharmacy, Minia University, Minia, Egypt.

**ARTICLE INFO**

Received on: 24/01/2023
Accepted on: 19/04/2023
Available Online: 04/07/2023

***Key words:***
Antitrypanosomal, metabolomics profiling, *Nephthea mollis*, *Trypanosoma brucei*, molecular docking, ornithine decarboxylase.

**ABSTRACT**

The crude extract and its derived ethyl acetate fraction of the soft coral *Nephthea mollis* displayed remarkable *in vitro* antitrypanosomal activity against *Trypanosoma brucei* with $IC_{50}$ values of 6.4 and 3.7 µg/ml, respectively. Consequently, the crude extract was subjected to LC–HR–ESI–MS metabolomics profiling to identify the constituents that may underlie their bioactivities. As a result, 33 secondary metabolites were characterized, among which sesquiterpenes and diterpenes prevailed. *In silico* molecular modeling revealed the high binding affinity for the ornithine decarboxylase active site, with five dereplicated compounds having docking scores higher than the cocrystallized ligand. These results highlight *N. mollis* as a rich source of compounds that might help develop therapies for Human African trypanosomiasis.

## INTRODUCTION

Human African trypanosomiasis (HAT) is one of the neglected tropical diseases that represent a serious threat to humans, especially in low-income countries of Africa, Asia, and South America (Molyneux *et al*., 2017). The geographical distribution of the sleeping sickness or HAT is restricted by a distribution of tsetse flies, which is found in the rural areas of more than 36 African countries (Brun and Blum, 2012; De Koning, 2020; Gayer *et al*., 2007). This vector-borne parasitic disease, caused by two subspecies of *Trypanosoma brucei* parasite: *Trypanosoma brucei gambiense* (accounts for 97% of cases) and *Trypanosoma brucei rhodesiense*, is considered fatal if left untreated (Pays, 1999; Steverding, 2010). Drug toxicities, resistance, and route of administration (either intramuscular and/or intravenous) raise the urgent need for new drugs orally effective against HAT (Álvarez-Bardón *et al*., 2020). Although extracts of natural products present many challenges to drug discovery programs worldwide (because of the chemical diversity found in a single extract), it is still known that bioactive compounds from natural products offer an incomparable and safer source for various disease therapies.

Moreover, the genus *Nephthea* has been reported to be rich in secondary metabolites such as sterols, sesquiterpenes, and diterpenes. Many of these metabolites recently showed

*Corresponding Author
*Khaled M. Allam, Department of Pharmacognosy, Faculty of Pharmacy, South Valley University, Qena, Egypt.*
*E-mail: khaled.mohamed @ svu.edu.eg*

antiprotozoal activities against various parasitic species such as trypanosome, malaria, and leishmania (Allam *et al*., 2021; Álvarez-Bardón *et al*., 2020).

Metabolomics is a valuable analytical tool used to comprehensively and highly accurately determine metabolites in a given metabolome (Bakr *et al*., 2021; Jacob *et al*., 2019; Said *et al*., 2021). It allows rapid identification (dereplication) and quantification of secondary metabolites in extracts. The combination of biological activity testing of crude extracts with metabolomics accelerates drug discovery, partly because crude extracts show higher biological activity and partly due to the ability to discriminate between complex mixtures of metabolites (Abdelmohsen *et al*., 2014; Kjer *et al*., 2010; Lotfy *et al*., 2021; Tawfike *et al*., 2013; Yuliana *et al*., 2011).

Ornithine decarboxylase (ODC), a proven drug target for the treatment of sleeping sickness, is the enzyme responsible for the metabolism of polyamines (such as putrescine, spermidine, and spermine) which are essential for cellular replication and hence parasite survival (Ibezim *et al*., 2017a). Trypanosome-specific metabolic and cellular pathways represent excellent molecular targets. The ability to synthesize polyamines, putrescine, and spermidine is vital for the proliferation of bloodstream forms in trypanosomes. In this process, ODC has a crucial function. This enzyme is considered the best-validated drug target in *T. brucei*, which is the target of eflornithine, a drug used clinically for treating HAT.

TTherefore, we aim to evaluate the in vitro antitrypanosomal activity of the crude extract and its derived fractions; petroleum ether and ethyl acetate of Nephthea mollis assisted by Liquid Chromatography-High Resolution-Electrospray Ionization - Mass Spectrometry (LC-HR-ESI-MS) metabolomics profiling to identify the secondary metabolites responsible for the antitrypanosomal potential of the soft coral. Additionally, we performed *in silico* molecular docking simulations within ODC active site to explore the binding mode of dereplicated compounds.

## MATERIAL AND METHODS

### Soft coral material

The soft coral *N. mollis* (Kingdom: Animalia, Phylum: Cnidaria, Class: Anthozoa, Subclass: Octocorallia, Order: Alcyonacea, Family: Nephtheidae) was collected by Prof. Mohamed A. Abu El-Regal, Professor of Biological Oceanography, Marine Biology Department, Faculty of Marine Science, King Abdulaziz University, Jeddah, Saudi Arabia, by scuba diving from the coasts of Hurghada, Egypt, at a depth of 12 m in March, 2018. It was then stored at −20°C ± 1°C until investigation. Part of the specimen used in the study was kept in the herbarium of the Pharmacognosy Department, Faculty of Pharmacy, Minia University, Minia, Egypt, under registration number Mn-Ph-Cog-47.

### Chemicals and reagents

Solvents used in this study (purchased from El-Nasr Company for Pharmaceuticals and Chemicals, Egypt), including ethanol, ethyl acetate, and petroleum ether (b.p. 60°C–80°C), were of analytical grade and distilled before use. Solvents of HPLC grade, such as acetonitrile and methanol, were obtained from SDFCL sd fine-Chem Limited, India. Suramin (Germanin®) was obtained from Bayer AG, Leverkusen, Germany.

### Extract preparation

The freeze-dried soft coral material (45 g) was extracted with ethanol until exhaustion. The crude ethanol extract (15 g, 33%) was suspended in distilled water and fractionated successively with petroleum ether and ethyl acetate. The organic phase in each step was separately concentrated under a vacuum, yielding the petroleum ether fraction (6 g), the ethyl acetate fraction (1 g), and the aqueous fraction (5 g). The crude extract and its derived fractions, petroleum ether and ethyl acetate, were kept at 4°C ± 1°C for antitrypanosomal assay and other analysis.

### *In vitro* antitrypanosomal assay

The antitrypanosomal activity was tested against *T. brucei* following the protocol of Huber and Koella (1993). A number of $10^4$ trypanosomes per milliliter of *T. brucei* strain TC 221 was cultivated in a complete Baltz medium. Trypanosomes were tested in 96-well plate chambers against different concentrations of test extracts (20 µL of stock solutions 10-200 µg/ml) diluted with 1 % Dimethyl Sulfoxide (DMSO) to a final volume of 200 µL. For control, 1% DMSO, as well as parasites without any test extracts, were used simultaneously in each plate to show an absence of any activity due to 1% DMSO. The plates were then incubated at 37°C ± 1 °C in an atmosphere of 5% $CO_2$ for 24 hours. After adding 20 µl of AlamarBlue, the activity was measured after 48 and 72 hours by light absorption using an MR 700 Microplate Reader at a wavelength of 550 nm with a reference wavelength of 650 nm. Linear interpolating three independent measurements quantified $IC_{50}$ values of the tested extracts. Suramin was used as a positive control ($IC_{50}$ 0.23 µg/ml) (Abdelmohsen *et al*., 2010; Cos *et al*., 2006).

### LC-MS metabolomics profiling

Metabolomics profiling of the crude extract of *N. mollis* was carried out as described by Abdelmohsen *et al.* (2010) (Elmaidomy *et al*., 2019) using an ACQUITY ultra-performance liquid chromatography system connected to a SYNAPT G2 HDMS quadrupole time-of-flight hybrid mass spectrometer (Waters, Milford, USA). Chromatographic separation was carried out using a BEH C18 column (2.1 × 100 mm, 1.7 µm particle size; Waters, Milford, USA) accompanied by a guard column (2.1 × 5 mm, 1.7 µm particle size). The mobile phase used during the separation consisted of purified water (A) and acetonitrile (B) with 0.1% formic acid added to each solvent. A gradient elution started at a flow rate of 300 µl/minute with 10% B linearly increasing to 100% B within 30 minutes and remaining isocratic for the next 5 minutes before linearly decreasing back to 10% B for the following 1 minute. The volume injected was 2 µl, and the column temperature was adjusted to 40°C ± 1°C. The obtained raw data were separated into positive and negative ionization modes using MSConvert software. Accordingly, the files were imported to the data mining software MZmine version 2.10 for peak picking, followed by deconvolution, deisotoping, alignment, and formula prediction. In MZmine, a framework for differential analysis of MS data, the RAW data are imported by selecting the ProteoWizard-converted positive or negative files in mzML format

followed by peaks detection in the sample using the chromatogram builder with a minimum time span set to 0.2 minutes, the minimum height and *m/z* tolerance to $1.0 \times 10^4$ and 0.001 *m/z* or 5.0 ppm, respectively. Mass ion peaks were isolated with a centroid detector threshold, greater than the noise level set to $1.0 \times 10^4$ and an MS level of one. For all remaining steps, select all files under peak lists before executing each step. Chromatogram deconvolution was then performed to detect the individual peaks. The local minimum search algorithm (chromatographic threshold: 95%, search minimum in RT range: 0.4 minutes, minimum relative height: 5%, minimum absolute height: $3.0 \times 10^4$, minimum ratio of peak top/edge: 3 and peak duration range: 0.2–5 minute) was applied. The isotopic peaks grouper was used (*m/z* tolerance: 0.001 *m/z* or 5.0 ppm, retention time tolerance: 0.1 absolute (minute), maximum charge: 2, and representative isotope: most intense) to identify the isotopes. This step will only deisotope peaks detected in the original search, i.e., those assigned a peak ID.

Filtering is helpful to set certain parameters when only considering a certain RT window, e.g., 5–40 minutes or *m/z* range window, or discard IDs that are only present in the sample. For chromatographic alignment and gap-filling, the retention time normalizer (*m/z* tolerance: 0.001 *m/z* or 5.0 ppm, retention time tolerance: 0.5 absolute (minute), and minimum standard intensity: $5.0 \times 10^3$) was used to reduce interbatch variation. The peak lists were all aligned using the join aligner parameters set to *m/z* tolerance: 0.001 *m/z* or 5.0 ppm, weight for *m/z*: 20, retention time tolerance: 5.0 relative (%), and weight for RT: 20. The values for the weight of *m/z* and RT should be kept the same; this means that both RT and *m/z* are given equal importance. Missing peaks were detected using the gap-filling peak finder with an intensity tolerance of 25%, *m/z* tolerance of 0.001 *m/z* or 5.0 ppm and retention time tolerance of 0.5 absolute (minute), followed by creating a file called "Neg-gap filled" if negative mode and "Pos-gap filled" if positive mode. An adduct search was performed for Na-H, K-H, $NH_4$, formate, and ACN+H (RT tolerance: 0.2 absolute (minute), *m/z* tolerance: 0.001 *m/z* or 5.0 ppm, max relative adduct peak height: 30%).

Additionally, a complex search was performed (ionization method: $[M+H]^+$ for ESI positive mode and $[M-H]^-$ for ESI negative mode, retention time tolerance: 0.2 absolute (minute), *m/z* tolerance: 0.001 *m/z* or 5.0 ppm and with a maximum complex peak height of 50%). The processed data set was then subjected to molecular formula prediction and peak identification to search for unidentified features and select atoms C, H, N, O, and other elements. Adjust parameters with heuristics element count with all three suboptions to get the isotope pattern filter working with all features with isotope peaks (Mahmoud *et al*., 2021).

Excel macros were written to enable the subtraction of background peaks. The Excel macro was used to dereplicate each *m/z* ion peak with compounds in the customized database (using RT and *m/z* threshold of ±3 ppm), which provided details on the putative identities of all metabolites. The macro was then utilized to identify the top 20 features (ranked by peak intensity) and to correspond putative identities in the sample by creating a list for the sample.

The Dictionary of Natural Products (DNP), METLIN, and MarinLit databases were used to identify compounds (Ancheeva *et al*., 2018).

### *In silico* molecular docking

*In silico* molecular docking simulations were performed for dereplicated compounds of *N. mollis* within the ODC (PDB ID: 1NJJ) active site. RCSB PDB deposited crystal structure resolution was 2.45 Å and it was used as a PDB entry for ODC since it was cocrystallized with a small molecule natural substrate capable of stimulating the activity of ODC in a biochemical and cell-based assay. Structures of dereplicated compounds were prepared in ChemDraw® Ultra (*v*. 8, 2013) and were transferred as smiles to Builder software embedded in Molecular Operating Environment (MOE 2014.0901; Chemical Computing Group, Montreal, QC, Canada) software. Protein-ligand complex was retrieved from the protein data bank, and the cocrystallized water molecules and nonessential small molecules were deleted. After carefully examining the topologies, the retained protein-ligand complex was subjected to energy minimization using GROMACS 4.5.5 and the GROMOS force field 53a6 (Berman *et al*., 2000; Scholz *et al*., 2015). The cocrystallized ligands were removed from the protein and redocked using the London dG scoring function implemented in MOE. Their structures were protonated at a cut-off value of 15 Å. Validation of the docking process of cocrystallized ligand (ornithine ORX) and MD simulations of all test compounds from *N. mollis* were done by the Triangle Matcher method, which was preferred because it has been reported to be more systematic in its ligand atoms alignment than other methods like Alpha Triangle. The poses generated from the placement stage were refined using the Forcefield refinement scheme according to its default settings. The scheme uses the molecular mechanics' setup and the reaction field functional form to perform energy minimization and treat the solvent effect (Ibezim 2017a, 2017b).

The free energy of binding of a given pose is estimated by the London dG scoring function from the sum of each of these terms: average gain/loss of rotational/translational entropy, energy due to loss of flexibility of the ligand, H-bond energies, energy due to metal-ligation and desolvation energy of atoms. London dG rescores 1 for only 10 retained docking poses of each compound, taking the lowest free energy of binding.

The resultant docking poses for each compound were examined and arranged according to their free binding energy value (S; Kcal/mol) and the root-mean-square deviation (RMSD; Å), using the lowest RMSD values relative to the crystal structure binding poses (Jackson *et al*., 2003; Shady *et al*., 2020).

## RESULTS AND DISCUSSION

### Antitrypanosomal activity

Using the protocol of Huber and Koella (1993), the crude extract, and its derived fractions, petroleum ether, and ethyl acetate of *N. mollis* were tested for their *in vitro* antitrypanosomal effects against *T. brucei*. The results revealed that the crude extract and ethyl acetate fraction of the soft coral *N. mollis* displayed remarkable *in vitro* antitrypanosomal effect against *T. brucei* with $IC_{50}$ values of 6.4 and 3.7 µg/ml, respectively, while the petroleum ether fraction shows a weak antitrypanosomal activity with $IC_{50}$ value of (>50 µg/ml). This encouraged us to undergo further metabolomics analysis of the active crude extract to reveal its constituents.

The proposed mechanism of action of sesquiterpenes in the parasite cells may be due to the formation of thiol adducts

with components found in the intracellular medium (namely trypanothione, glutathione, and thiol groups in proteins). The parasite's cells become more vulnerable to oxidative stress with a reduction in trypanothione and, hence, it was suggested that compounds induced programmed cell death in the tested parasite (Zeouk *et al*., 2020). In another way, the proposed mechanism of action of diterpenes in the parasite cells may be due to their considerable permeabilization in the membrane of the parasite (Ueno *et al*., 2018).

**Metabolomics analysis**

The crude extract of *N. mollis* was subjected to metabolomics profiling for the first time. The chemical profiling of dereplicated compounds was consistent with literature data on secondary metabolites of *N. mollis* (Figs. 1 and 2). The dereplicated compounds were identified using databases (DNP, METLIN, and MarinLit databases) (Macintyre *et al*., 2014). Thirty-three compounds were preliminarily identified based on their mass and summarized in Table 1 and Figure 3. Most of the identified

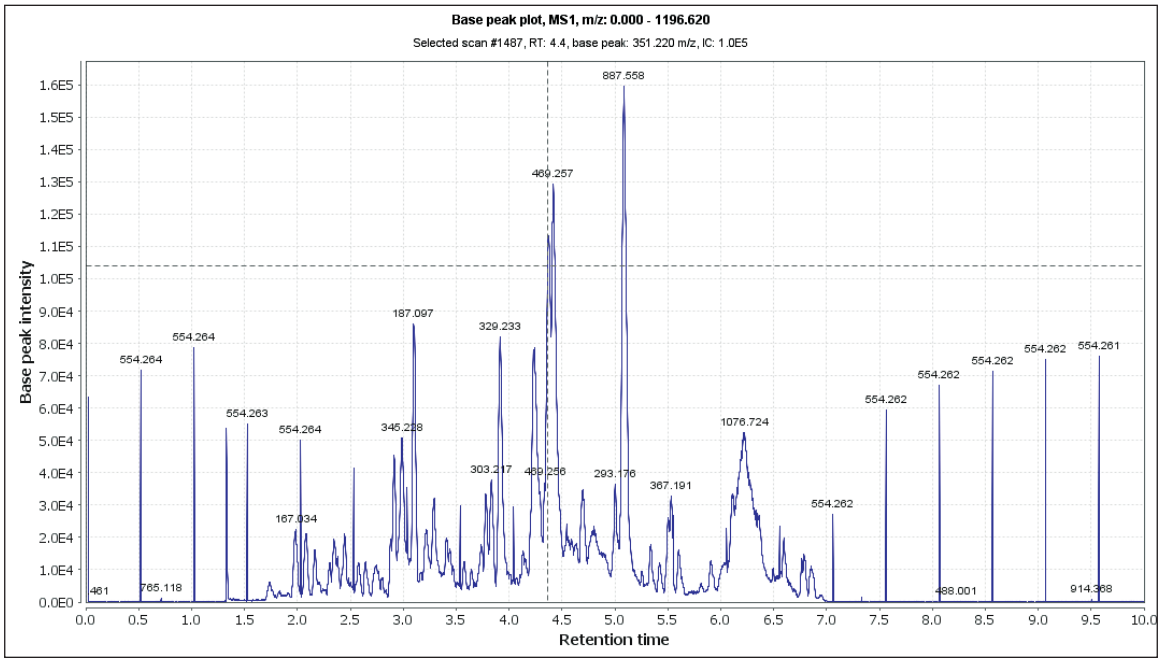


**Figure 1.** Total ion chromatogram of the crude extract of *N. mollis* (negative mood).

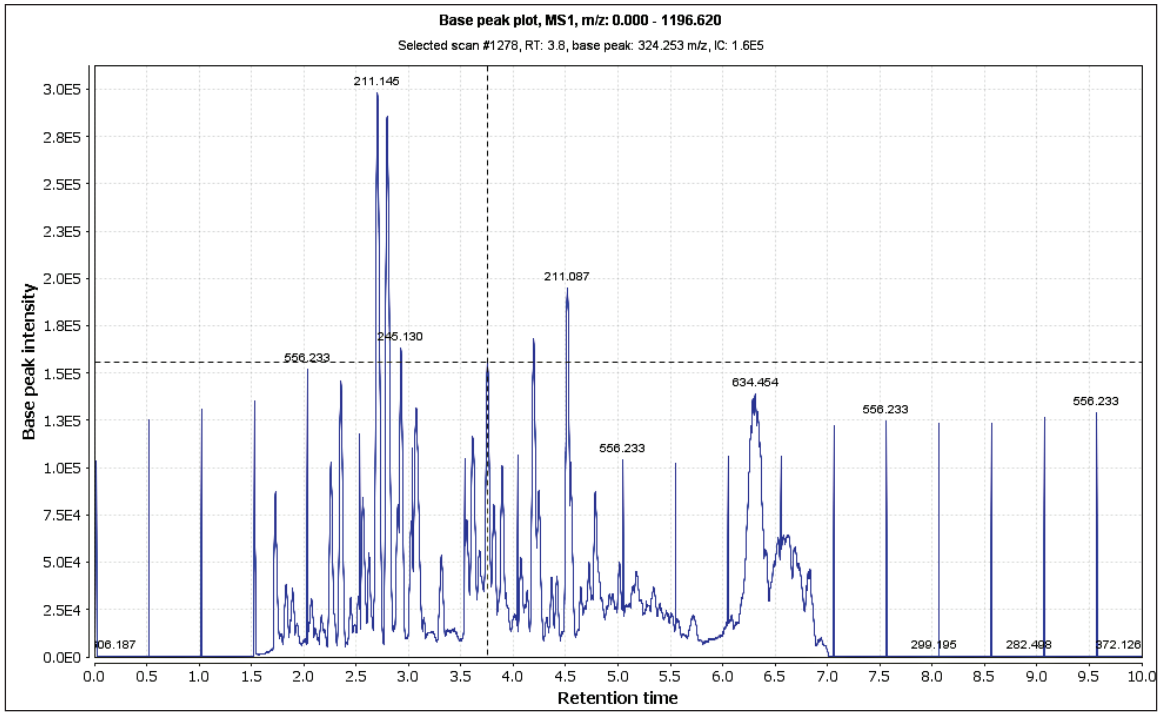


**Figure 2.** Total ion chromatogram of the crude extract of *N. mollis* (positive mood).

**Table 1.** A list of identified metabolites in soft coral *N. mollis*.

| # | Putative identified | Class | Rt | *m/z* | Molecular formula | Source |
|---|---|---|---|---|---|---|
| 1 | Cadina-4(14),5-diene | Sesquiterpenes | 6.12 | 204.1875 | $C_{15}H_{24}$ | *Nephthea sp.* |
| 2 | 4,15-Dihydroguaian-6,10-diene | Sesquiterpenes | 6.12 | 204.1879 | $C_{15}H_{24}$ | *Nephthea chabrolii* |
| 3 | Eudesma-4,7(11)-diene-8*β*-ol | Sesquiterpenes | 4.73 | 220.183 | $C_{15}H_{24}O$ | *Nephthea chabrolii* |
| 4 | Guaianediol | Sesquiterpenes | 4.73 | 220.183 | $C_{15}H_{24}O$ | *Nephthea chabrolii* |
| 5 | 1*S*,4*R*,5*S*-Guia-6,9-dien-4-ol | Sesquiterpenes | 4.73 | 220.183 | $C_{15}H_{24}O$ | *Nephthea chabrolii* |
| 6 | 3,4-Epoxyguaia-10(12)-ene | Sesquiterpenes | 4.73 | 220.183 | $C_{15}H_{24}O$ | *Nephthea sp.* |
| 7 | Guaian-4,6-dien-10*α*-ol | Sesquiterpenes | 4.73 | 220.183 | $C_{15}H_{24}O$ | *Nephthea chabrolii* |
| 8 | 8*β*-Hydroxyprespatane | Sesquiterpenes | 4.73 | 220.183 | $C_{15}H_{24}O$ | *Nephthea erecta* |
| 9 | Capillosanol | Ssquiterpenes | 4.73 | 220.183 | $C_{15}H_{24}O$ | *Nephthea chabrolii* |
| 10 | 1*α*-Hydroxy-(+)-cyclocolorenone | Sesquiterpenes | 2.99 | 234.1614 | $C_{15}H_{22}O_2$ | *Nephthea* sp. |
| 11 | Hydroxycolorenone | Sesquiterpenes | 2.99 | 236.1774 | $C_{15}H_{24}O_2$ | *Nephthea chabrolii* |
| 12 | 6*β*,7*β*-Epoxy-4*β*-hydroxyguian-10-ene | Sesquiterpenes | 2.99 | 236.1774 | $C_{15}H_{24}O_2$ | *Nephthea chabrolii* |
| 13 | 3,4-Epoxy-11-hydroxy-1-pseudoguaiene | Sesquiterpenes | 2.99 | 236.1774 | $C_{15}H_{24}O_2$ | *Nephthea erecta* |
| 14 | 8*β*-Hydroperoxyprespatane | Sesquiterpenes | 2.99 | 236.1774 | $C_{15}H_{24}O_2$ | *Nephthea erecta* |
| 15 | Charolidione A | Sesquiterpenes | 2.99 | 236.1774 | $C_{15}H_{24}O_2$ | *Nephthea chabrolii* |
| 16 | (2*E*,6*E*)-3-Isopropyl-6-methyl-10-oxoundec-2,6-dienal | Sesquiterpenes | 2.99 | 236.1774 | $C_{15}H_{24}O_2$ | *Nephthea erecta* |
| 17 | Ent-oplopanone | Sesquiterpenes | 4.72 | 238.1934 | $C_{15}H_{26}O_2$ | *Nephthea sp.* |
| 18 | Nephthediol | Sesquiterpenes | 4.72 | 238.1934 | $C_{15}H_{26}O_2$ | *Nephthea sp.* |
| 19 | Chabranol | Sesquiterpenes | 4.50 | 240.1727 | $C_{14}H_{24}O_3$ | *Nephthea chabrolii* |
| 20 | Methoxycolorenone | Sesquiterpenes | 5.21 | 250.1932 | $C_{16}H_{26}O_2$ | *Nephthea chabrolii* |
| 21 | 2-Deoxy-7-*O*-methyllemnacarnol | Sesquitepenes | 5.21 | 250.1932 | $C_{16}H_{26}O_2$ | *Nephthea sp.* |
| 22 | 10*α*-Methoxy-4*β*-hydroxy guaian-6-ene | Sesquiterpenes | 5.01 | 252.2085 | $C_{16}H_{28}O_2$ | *Nephthea chabrolii* |
| 23 | Nephtheoxydiol | Sesquiterpenes | 5.11 | 254.1878 | $C_{15}H_{26}O_3$ | *Nephthea sp.* |
| 24 | 1*S*-Acetoxygermacra-3*Z*,5*E*,10(15)-triene | Ssquiterpenes | 5.41 | 262.1932 | $C_{17}H_{26}O_2$ | *Nephthea chabrolii* |
| 25 | Armatin E | Sesquiterpenes | 5.41 | 264.1718 | $C_{16}H_{24}O_3$ | *Nephthea aramata* |
| 26 | 4*α*-*O*-Acetyl-selin-11-en | Sesquiterpenes | 5.41 | 264.2088 | $C_{17}H_{28}O_2$ | *Nephthea brassica* |
| 27 | 2-Deoxy-12-ethoxy-7-*O*-methyl lemnacarnol | esquiterpenes | 5.99 | 294.2187 | $C_{18}H_{30}O_3$ | *Nephthea* sp. |
| 28 | Ketochabrolic acid | Terpenoid-related C.A. | 2.95 | 292.2032 | $C_{18}H_{28}O_3$ | *Nephthea chabrolii* |
| 29 | Isoketochabrolic acid | Terpenoid-related C.A. | 2.95 | 292.2032 | $C_{18}H_{28}O_3$ | *Nephthea chabrolii* |
| 30 | Chabrolol A | Diterpenes | 5.41 | 264.2088 | $C_{17}H_{28}O_2$ | *Nephthea chabrolii* |
| 31 | Brassicolide | Diterpenes | 5.65 | 318.2202 | $C_{20}H_{30}O_3$ | *Nephthea brassica* |
| 32 | Brassicolene | Diterpenes | 5.73 | 328.2408 | $C_{22}H_{32}O_2$ | *Nephthea brassica* |
| 33 | Nephthenol | Diterpenes | 2.99 | 290.260 | $C_{20}H_{34}O$ | *Nephthea* sp. |

compounds (27 compounds) were identified as sesquiterpenes type of compounds, in addition to a few diterpenes and terpenoid-related carboxylic acids compounds.

The mass ion peak at *m/z* 204.187 for the suggested formula $C_{15}H_{24}$ was identified as cadina-4(14),5-diene (**1**), which was formerly reported from the soft coral *Nephthea* sp. (Kitagawa *et al*., 1987). Likewise, the mass ion peak at *m/z* 204.187 for the predicted molecular formula $C_{15}H_{24}$ was also dereplicated as the sesquiterpene: 4,15-dihydro guaian-6,10-diene (**2**), which was previously obtained from *Nephthea chabrolii* (Amir *et al*., 2012). Additionally, the mass ion peak at *m/z* 220.183, in accordance with the molecular formula $C_{15}H_{24}O$, was dereplicated as eudesma-4,7(11)-diene-8*β*-ol (**3**) and/or guaianediol (**4**) and/or 1*S*,4*R*,5*S*-guia-6,9-dien-4-ol (**5**) and/or 3,4-epoxyguaia-10 (12)-ene (**6**) and/or guaian-4,6-dien-10*α*-ol (**7**) and/or 8*β*-hydroxyprespatane (**8**) and/or capillosanol (**9**). All of these sesquiterpenes were previously obtained from *N. chabrolii* (Amir *et al*., 2012) except sesquiterpenes (**6**) and (**8**) which were obtained from *Nephthea* sp. and *Nephthea erecta*, respectively (Amir *et al*., 2012) Similarly, the mass ion peak at *m/z* 234.161 for the predicted molecular formula $C_{15}H_{22}O_2$ was dereplicated as the sesquiterpenes: 1*α*-hydroxy-(+)-cyclocolorenone (**10**), which was formerly characterized from *Nephthea* sp. (Hu *et al*., 2011). Furthermore, the mass ion peak at *m/z* 236.177, in accordance with the molecular formula $C_{15}H_{24}O_2$, was dereplicated as hydroxycolorenone (**11**) and/or 6*β*,7*β*-epoxy-4*β*-hydroxyguaian-10-ene (**12**) and/or 3,4-epoxy-11-hydroxy-1-pseudoguaiene (**13**) and/or 8*β*–hydroperoxyprespatane (**14**) and/or chabrolidione A (**15**) and/or (2*E*,6*E*)-3-isopropyl-6-methyl-10-oxoundec-2,6-dienal (**16**). Sesquiterpenes (**11**), (**12**), and (**15**) were previously

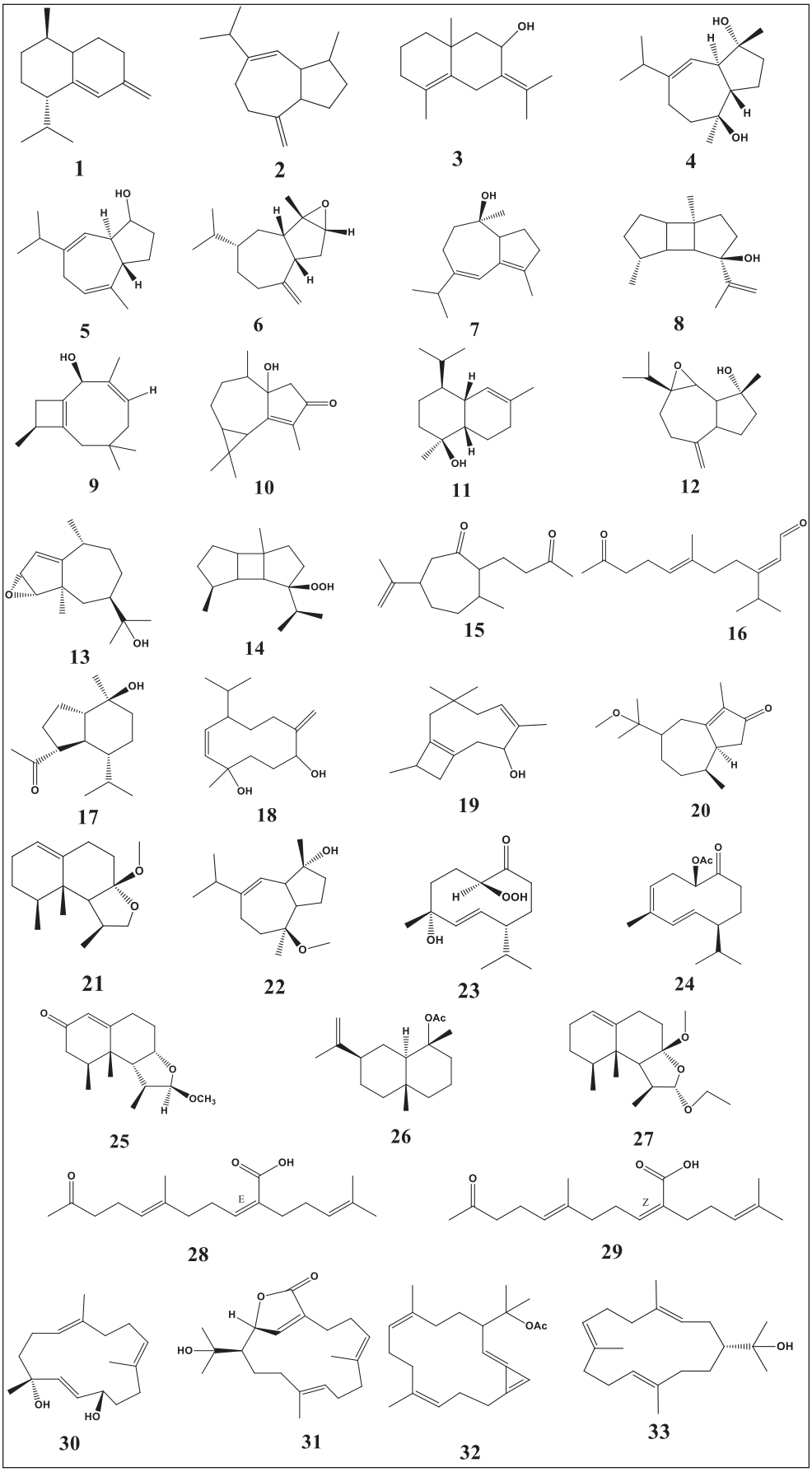


**Figure 3.** Chemical structure of dereplicated compounds **1–33.**

**Table 2.** Binding free energy (S; kcal/mol) and binding accuracy (RMSD; Å) of *N. mollis* and cocrystallized ligand within ODC active site (PDB ID: 1NJJ).

| Molecule | Docking score (S; kcal/mol) | RMSD (Å) |
|---|---|---|
| INJJ cocrystallized ligand (ORX) | −4.5058 | 1.8918 |
| 2-Deoxy-12-ethoxy-7-*O*-methyl lemnacarnol | −5.2186 | 2.0242 |
| Nephthenol | −4.8930 | 1.8370 |
| 4*α*-*O*-Acetyl-selin-11-en | −4.6440 | 1.9708 |
| Eudesma-4,7(11)-diene-8*β*-ol | −4.5653 | 0.6331 |
| Chabrolidione A | −4.5278 | 0.9897 |
| Guaian-4,6-dien-10*α*-ol | −4.4267 | 1.6648 |
| Brassicolide | −4.4262 | 1.8294 |
| Capillosanol | −4.2383 | 2.2662 |
| Chabrolol A | −4.2271 | 1.8498 |
| Nephtheoxydiol | −4.1673 | 1.4596 |
| 1*α*-Hydroxy-(+)-cyclocolorenone | −4.0963 | 1.3961 |
| 1*S*-Acetoxygermacra-3*Z*,5*E*,10(15)-triene | −4.0880 | 0.9902 |
| 8*β*-Hydroperoxyprespatane | −4.0673 | 1.5743 |
| 3,4-Epoxyguaia-10(12)-ene | −4.0394 | 1.7450 |
| 2-Deoxy-7-*O*-methyllemnacarnol | −4.0057 | 1.4953 |
| 4,15-Dihydroguaian-6,10-diene | −3.9922 | 1.9155 |
| 10*α*-Methoxy-4*β*-hydroxy guaian-6-ene | −3.9431 | 1.8772 |
| 8*β*-Hydroxyprespatane | −3.8998 | 1.5906 |
| 6*β*,7*β*-Epoxy-4*β*-hydroxyguaian-10-ene | −3.8558 | 2.0234 |
| Methoxycolorenone | −3.7555 | 2.1270 |
| Chabranol | −3.7507 | 1.6197 |
| Hydroxycolorenone | −3.5285 | 2.1016 |
| Nephthediol | −3.4163 | 2.4168 |
| Cadina-4(14),5-diene | −3.4067 | 2.4022 |
| Armatin E | −3.3336 | 2.1020 |
| Ent-oplopanone | −2.8246 | 2.3728 |
| Brassicolene | −2.7567 | 2.5090 |
| 1*S*,4*R*,5*S*-Guia-6,9-dien-4-ol | −2.0255 | 1.1860 |

obtained from *N. chabrolii* (Hu *et al*., 2011; Su *et al*., 2007), while sesquiterpenes (**13**), (**14**), and (**16**) were obtained from *N. erecta* (Abdelhafez *et al*., 2020). Moreover, the mass ion peak at *m/z* 238.193, in agreement with the molecular formula $C_{15}H_{26}O_2$ was dereplicated as sesquiterpenes; ent-oplopanone (**17**) and/or nephthediol (**18**) both were previously reported from *Nephthea* sp. (Kitagawa *et al*., 1987). Similarly, the mass ion peak at *m/z* 240.172 for the predicted molecular formula $C_{14}H_{24}O_3$, was dereplicated as the sesquiterpenes; chabranol (**19**) was formerly characterized from *N. chabrolii* (Amir *et al*., 2012). Moreover, the mass ion peak at *m/z* 250.193, in agreement with the molecular formula $C_{16}H_{26}O_{2,}$ was dereplicated as the sesquiterpenes. As for methoxycolorenone (**20**) and/or 2-deoxy-7-*O*-methyllemnacarnol (**21**), the former was previously reported from *N. chabrolii* (Handayani *et al*., 1997), while the latter was previously reported from *Nephthea* sp. (Kapojos *et al*., 2008). Another compound was dereplicated as 10*α*-methoxy-4*β*-hydroxy guaian-6-ene (**22**), on account of the observed mass ion peak at *m/z* 252.208 and in accordance with the molecular formula $C_{16}H_{28}O_2$. This sesquiterpene was formerly characterized from *N. chabrolii* (Amir *et al*., 2012). Additionally, the mass ion peak at *m/z* 254.187 for the suggested formula $C_{15}H_{26}O_3$ was identified as nephtheoxydiol (**23**). These sesquiterpenes were formerly reported from the soft coral *Nephthea* sp. (Kitagawa *et al*., 1987). Likewise, the mass ion peak at *m/z* 262.193 for the predicted molecular formula $C_{17}H_{26}O_2$ was dereplicated as the sesquiterpenes: 1*S*-acetoxygermacra-3*Z*,5*E*,10(15)-triene (**24**), which was previously characterized from *N. chabrolii* (Zhang *et al*., 2001). Similarly, the mass ion peak at *m/z* 264.171, in consonance with the predicted formula $C_{16}H_{24}O_3$, was dereplicated as armatin E (**25**), a sesquiterpene earlier reported in *Nephthea armata* (El-Gamal *et al*., 2004), while that at *m/z* 264.208 was characterized as 4*α*-*O*-acetyl-selin-11-en (**26**), a sesquiterpene having the molecular formula $C_{17}H_{28}O_2$. This compound was identified from *Nephthea brassica* (Duh *et al*., 1999). The mass ion peak at *m/z* 294.218 for the predicted molecular formula $C_{18}H_{30}O_3$ was dereplicated as the sesquiterpenes: 2-deoxy-12-ethoxy-7-*O*-methyl lemnacarnol (**27**), which was previously characterized from *Nephthea* sp. (Kapojos *et al*., 2008). Besides the sesquiterpenes constituents, an assortment of other structurally different metabolites has also been described encompassing terpenoid-related carboxylic acids: ketochabrolic acid (**28**) and/or isoketochabrolic acid (**29**), which were identified from the mass

ion peak at *m/z* 292.203, in agreement with the molecular formula $C_{18}H_{28}O_3$. Both compounds were previously reported from *N. chabrolii* (Su *et al*., 2007). Moreover, as a common biosynthetic feature of *Nephthea* soft corals, LC-HR-ESI-MS analysis indicated the presence of a variety of diterpenes. In that respect, the mass ion peak at *m/z* 264.208, consistent with the formula $C_{17}H_{28}O_2$, was dereplicated as chabrolol A (**30**) that was previously identified from *N. chabrolii* (Zhang *et al*., 2001). Likewise, the mass ion peak at *m/z* 318.220 for the suggested molecular formula $C_{20}H_{30}O_3$ was characterized as brassicolide (**31**), while that at *m/z* 328.240 for the suggested molecular formula $C_{22}H_{32}O_2$ was characterized as brassicolene (**32**), and both diterpenes (**31**) and (**32**) were formerly obtained from *N. brassica* (Duh *et al*., 1999). Another diterpene with the molecular formula $C_{20}H_{34}O$, in good agreement with the mass ion peak at *m/z* 290.260, was characterized as nephthenol (**33**), which was previously reported from *Nephthea* sp. (Kitagawa *et al*., 1987).

## Molecular docking

For further exploration and to get a better idea about the possible target affected by dereplicated compounds of *N. mollis* to afford their antitrypanosomal activity, we performed *in silico* molecular docking simulations within ODC. The X-ray structure of ODC showed ligands; D-ornithine, ORX, a substrate analog, was placed within the ODC active site, and Geneticin (G418) as a weak non-competitive inhibitor occupying an allosteric site of ODC. Molecular docking simulations performed within the active site of ODC showed a number of binding interactions (H-bonding and H-pi interactions) between ORX and a number of amino acid residues (GLU 274, ASP 332, GLY 276, ARG 277, TYR 389, GLY 237, and HIS 197) with binding free energy (expressed as docking score, S) of −4.5058 kcal/mol, as listed in Table 2.

Docking of dereplicated compounds within ODC active site revealed a number of interesting observations. First of all, binding free energy for five of the identified compounds (2-deoxy-12-ethoxy-7-o-methyl lemnacarnol, nephthenol, 4*α*-o-acetyl-selin-11-en, eudesma-4,7(11)-diene-8*β*-ol, and chabrolidione A) was better than ORX, as listed in Table 2.

Additionally, as found with ORX, most of the test compounds showed either H-bonding and/or H-pi binding interactions with key amino acid residues: GLU 274, ARG 277, and HIS 197 (Table 3 and Fig. 4). Finally, a visual inspection of the best docking poses of 6,7-epoxy-4-hydroxyguaian-10-ene, chabrolidione A, and nephtheoxydiol showed a good overlay with ORX within ODC active site, as shown in Figure 5. Overall, the docking results showed how good the overlay of the dereplicated compounds of *N. mollis* with ORX within ODC active site was, which could be used for explaining their antitrypanosomal activity.

**Table 3**. Binding free energy (S; kcal/mol) and binding interactions for co-crystallized ligand (ORX) and Nephthea mollis within ornithine decarboxylase (ODC) active site (PDB ID: 1NJJ; 2.45 Å).

| Ligand | Binding energy score (S; kcal/mol) | Active site interactions | | |
|---|---|---|---|---|
| | | a. a. residue | Bond type | Bond length (Å) |
| Cocrystallized ligand (ORX) | −4.5058 | GLU 274 | H-donor | 3.16 |
| | | ASP 332 | H-donor | 3.30 |
| | | GLY 276 | H-acceptor | 2.92 |
| | | ARG 277 | H-acceptor | 2.74 |
| | | TYR 389 | H-acceptor | 2.55 |
| | | GLY 237 | H-acceptor | 2.70 |
| | | GLY 276 | H-acceptor | 3.07 |
| | | TYR 389 | H-pi | 3.71 |
| | | HIS 197 | Pi-pi | 3.88 |
| 8*β*-Hydroxyprespatane | −3.8998 | ARG 154 | H-acceptor | 2.91 |
| | | ARG 154 | H-acceptor | 3.17 |
| Capillosanol | −4.2383 | HIS 197 | H-pi | 4.36 |
| 1*α*-Hydroxy-(+)-cyclocolorenone | −4.0963 | HIS 197 | H-pi | 3.98 |
| Hydroxycolorenone | −3.5285 | LYS 69 | H-acceptor | 3.11 |
| 6*β*,7*β*-Epoxy-4*β*-hydroxyguaian-10-ene | −3.8558 | LYS 69 | H-acceptor | 2.95 |
| | | HIS 197 | H-pi | 3.97 |
| 8*β*-Hydroperoxyprespatane | −4.0673 | LYS 69 | H-acceptor | 3.31 |
| Chabranol | −3.7507 | ARG 277 | H-acceptor | 2.91 |
| | | HIS 197 | H-pi | 3.85 |
| Chabrolidione A | −4.5278 | LYS 69 | H-acceptor | 2.94 |
| | | ARG 277 | H-acceptor | 2.92 |
| | | SER 200 | H-acceptor | 3.06 |
| 1*S*-Acetoxygermacra-3*Z*,5*E*,10(15)-triene | −4.0880 | GLU 274 | H-donor | 3.31 |
| Chabrolol A | −4.2271 | GLU 274 | H-donor | 2.71 |
| Nephthenol | −4.8930 | ARG 277 | H-acceptor | 2.79 |
| Nephthediol | −3.4163 | LYS 69 | H-acceptor | 3.26 |

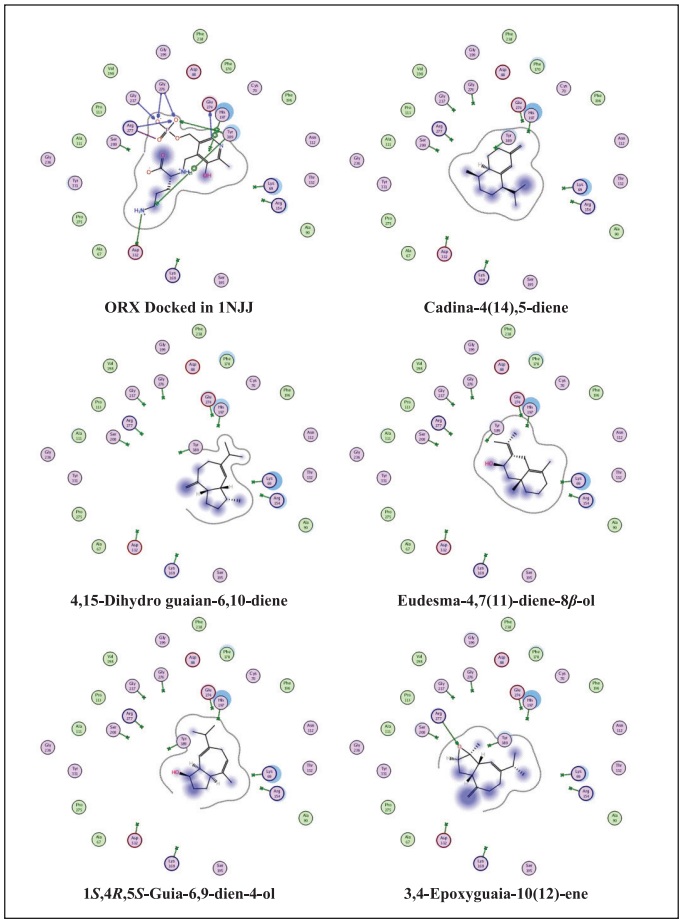
ORX Docked in 1NJJ
Cadina-4(14),5-diene
4,15-Dihydro guaian-6,10-diene
Eudesma-4,7(11)-diene-8β-ol
1S,4R,5S-Guia-6,9-dien-4-ol
3,4-Epoxyguaia-10(12)-ene

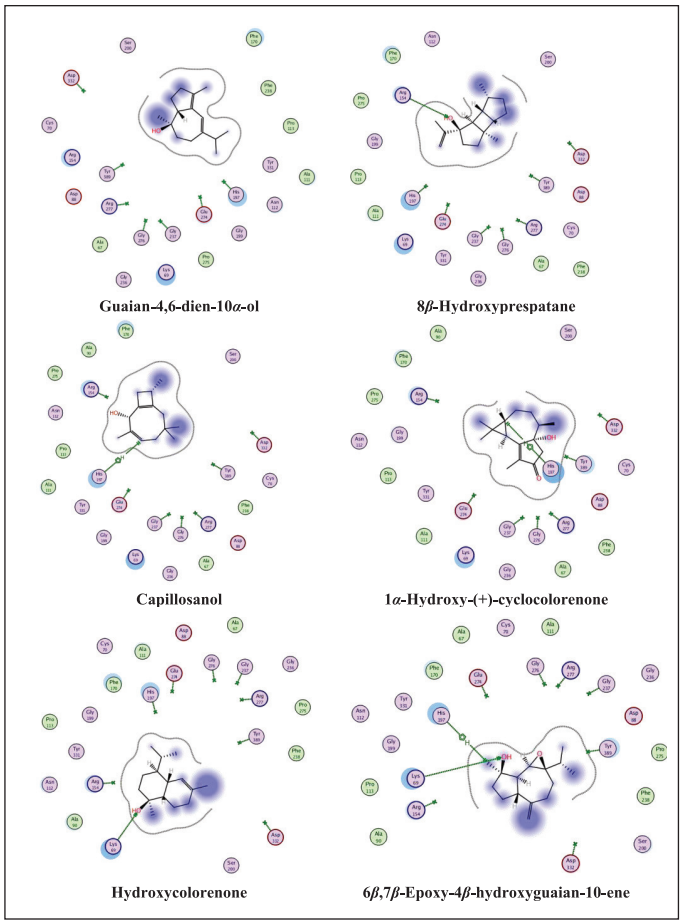
Guaian-4,6-dien-10α-ol
8β-Hydroxyprespatane
Capillosanol
1α-Hydroxy-(+)-cyclocolorenone
Hydroxycolorenone
6β,7β-Epoxy-4β-hydroxyguaian-10-ene

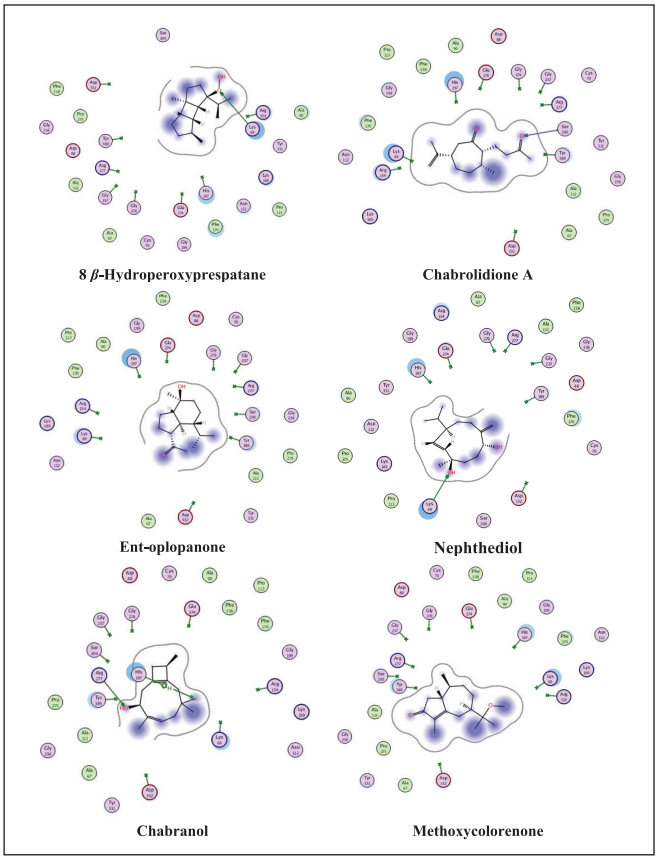
8 β-Hydroperoxyprespatane
Chabrolidione A
Ent-oplopanone
Nephthediol
Chabranol
Methoxycolorenone

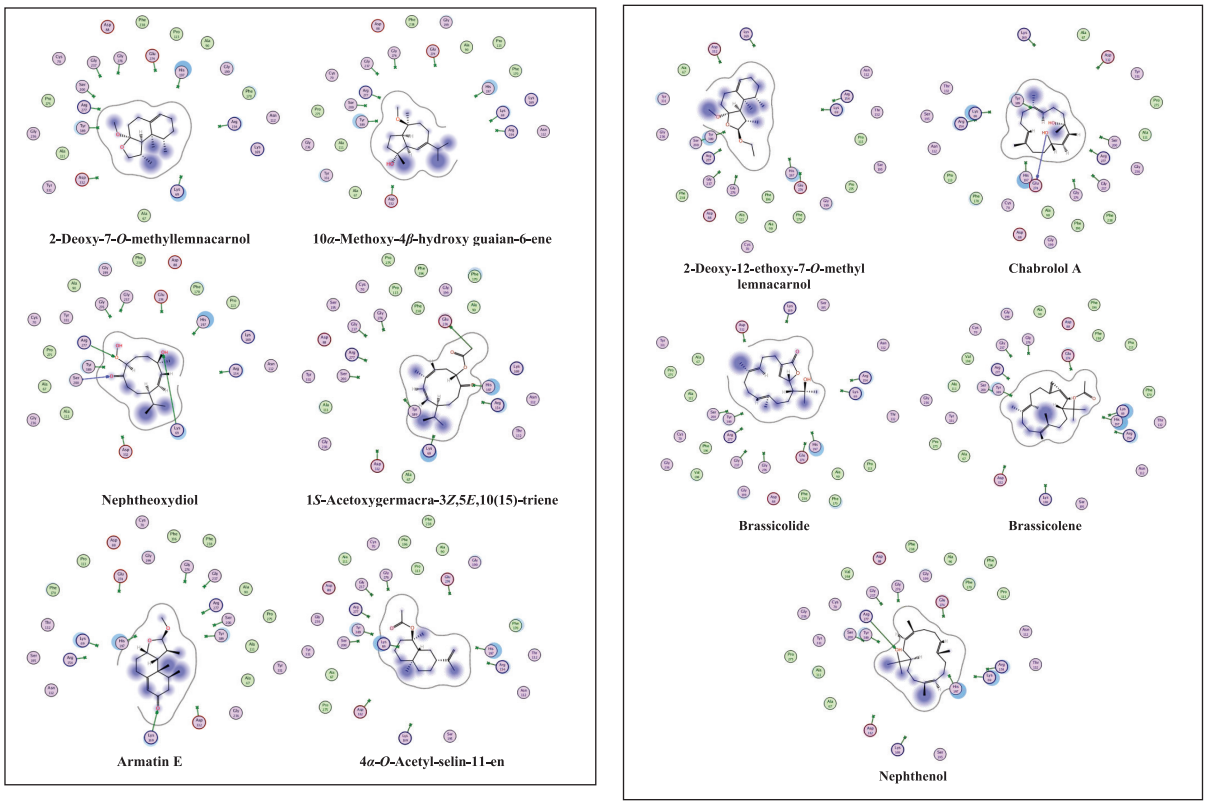


**Figure 4.** 2D interaction diagrams in the active site 1NJJ made by the cocrystallized ligand (ORX) and the dereplicated compounds. The MOE software generates the diagrams.

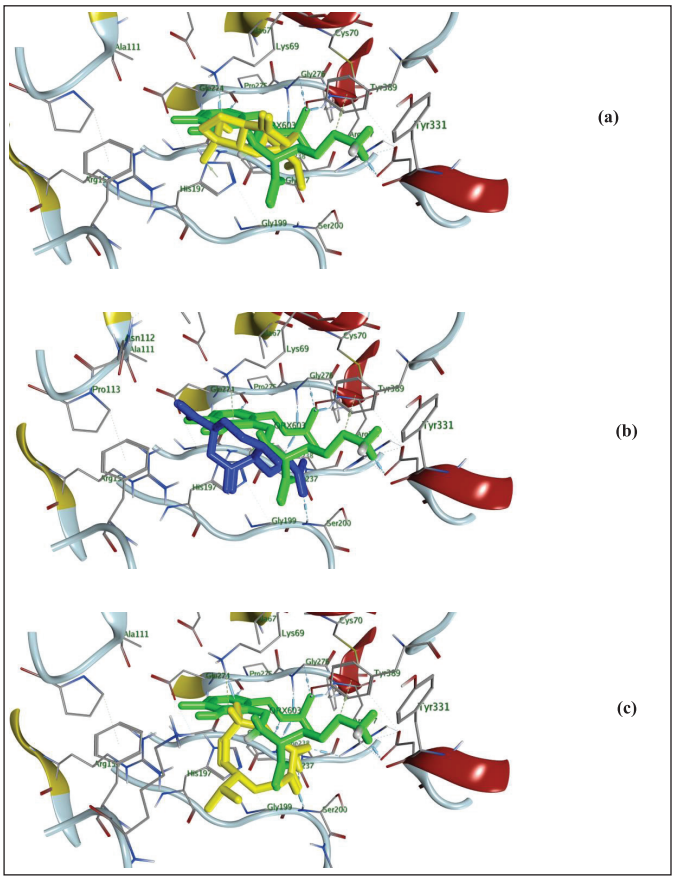


**Figure 5.** 3D presentation of 6,7-epoxy-4-hydroxyguaian-10-ene (yellow-color; (a), chabrolidione A blue-color; (b), nephtheoxydiol yellow-color; (c) overlay within 1NJJ active site and its ligand (ORX; green-color).

## CONCLUSION AND FUTURE PERSPECTIVES

This study highlighted the promising antitrypanosomal activity of the soft coral *N. mollis* extracts as a possible natural therapy for HAT. The crude extract and its derived ethyl acetate fraction displayed remarkable *in vitro* antitrypanosomal activity against *T. brucei*. Thirty-three compounds of sesquiterpenes and diterpenes class of compounds were mined with the help of LC–MS-based metabolomics. Docking studies within ODC crystal structure provided insights about how the dereplicated compounds bind and interact with various amino acid residues lining ODC active site, which was further evidenced by *in vitro* assays against *T. brucei*. Thus, further work on the extract of *N. mollis* will be included in our plans to purify the compounds responsible for their antitrypanosomal activity and perform *in vivo* experiments and safety studies for the purified compounds. Moreover, it should be further investigated for a supportive role in the pharmaceutical field toward developing new antitrypanosomal drugs.

## ACKNOWLEDGMENTS

We thank Prof. RuAngelie Edrada-Ebel (Head of the Natural Products Metabolomics Group, University of Strathclyde) for the Macro software used in the dereplication study. The authors uploaded the article on the preprint server link here: https://assets.researchsquare.com/files/rs-1090567/v1/779390fd-82d0-4c1b-b8e1 49f8261e3005.pdf?c=1637766316; DOI: https://doi.org/10.21203/rs.3.rs-1090567/v1. The authors will inform the preprint server after the publication of this article in JAPS.

## CONFLICTS OF INTEREST

The authors reported no potential conflicts of interest.

## FUNDING

There is no funding to report.

## ETHICAL APPROVALS

This study does not involve experiments on animals or human subjects.

## DATA AVAILABILITY

All data generated and analyzed are included in this research article.

## PUBLISHER'S NOTE

This journal remains neutral concerning jurisdictional claims in published institutional affiliation.

## AUTHORS' CONTRIBUTIONS

K.M.A. did conceptualization, data curation, and writing-original draft. Y.A.M. did formal analysis and methodology. U.R.A. carried out writing review and editing. A.I.K. did investigation, A.E.A. validation, M.A.F. project administration, and E.S.E. supervision. All authors discussed the results and contributed to the final manuscript.

## REFERENCES

Abdelhafez OH, Ali TFS, Fahim JR, Desoukey SY, Ahmed S, Behery FA, Kamel MS, Gulder TA, Abdelmohsen UR. Anti-inflammatory potential of green synthesized silver nanoparticles of the soft coral *Nephthea* sp. supported by metabolomics analysis and docking studies. Int J Nanomed, 2020; 15(1):5345–60.

Abdelmohsen UR, Cheng C, Viegelmann C, Zhang T, Grkovic T, Ahmed S, Quinn RJ, Hentschel U, Edrada-Ebel RJMd. Dereplication strategies for targeted isolation of new antitrypanosomal actinosporins A and B from a marine sponge associated-*Actinokineospora* sp. EG49. Mar Drugs, 2014; 12(3):1220–44.

Abdelmohsen UR, Pimentel-Elardo SM, Hanora A, Radwan M, Abou-El-Ela SH, Ahmed S, Hentschel UJ. Isolation, phylogenetic analysis and anti-infective activity screening of marine sponge-associated *Actinomycetes*. Mar Drugs, 2010; 8(3):399–412.

Allam KM, Khedr AI, Allam AE, Abdelkader MSA, Elkhayat ES, Fouad MA. Chemical, and biological diversity in *Nephthea* soft corals in the current decade: a review. JABPS, 2021; 4(3):124–33.

Álvarez-Bardón M, Pérez-Pertejo Y, Ordóñez C, Sepúlveda-Crespo D, Carballeira NM, Tekwani BL, Murugesan S, Martinez-Valladares M, García-Estrada C, Reguera RMJMD. Screening marine natural products for new drug leads against trypanosomatids and malaria. Mar Drugs, 2020; 18(4):187.

Amir F, Koay YC, Yam WS. Chemical constituents and biological properties of the marine soft coral *Nephthea*: a review (Part 1). Trop J Pharm Res, 2012; 11(3):485–98.

Ancheeva E, Daletos G, Proksch P. Lead compounds from mangrove-associated microorganisms. Mar Drugs, 2018; 16(9):319.

Bakr RO, Tawfike A, El-Gizawy HA, Tawfik N, Abdelmohsen UR, Abdelwahab MF, Alshareef WA, Fayez SM, El-Mancy SM, El-Fishawy AM, Abdelkawy MA, Fayed MA. The metabolomic analysis of five *Mentha* species: cytotoxicity, anti-helicobacter assessment, and the development of polymeric micelles for enhancing the anti-helicobacter activity. RSC Adv, 2021; 11(13):7318–30.

Berman HM, Westbrook J, Feng Z, Gilliland G, Bhat TN, Weissig H, Shindyalov IN, Bourne PE. The protein data bank. Nucl Acids Res, 2000; 28(1):235–42.

Brun R, Blum J. Human African trypanosomiasis. Infect Dis Clin, 2012; 26(2):261–73.

Cos P, Vlietinck AJ, Berghe DV, Maes L. Anti-infective potential of natural products: how to develop a stronger *in vitro* proof-of-concept'. J Ethnopharmacol, 2006; 106(3):290–302.

De Koning PH. The drugs of sleeping sickness: their mechanisms of action and resistance, and a brief history. Trop Med Infect Dis, 2020; 5(1):14.

Duh CY, Wang SK, Weng YL, Chiang MY, Dai FJ. Cytotoxic terpenoids from the Formosan soft coral *Nephthea brassica*. J Nat Prod, 1999; 62(11):1518–21.

El-Gamal AA, Wang SK, Dai CF, Duh CY. New nardosinanes and 19-oxygenated ergosterols from the soft coral *Nephthea armata* collected in Taiwan. J Nat Prod, 2004; 67(9):1455–8.

Elmaidomy AH, Mohammed R, Hassan HM, Owis AI, Rateb ME, Khanfar MA, Krischke M, Mueller MJ, Abdelmohsen UR. Metabolomic profiling and cytotoxic tetrahydrofurofuran lignans investigations from *Premna odorata Blanco*. Metabolites, 2019; 9(10):223.

Gayer M, Legros D, Formenty P, Connolly MA. Conflict and emerging infectious diseases. Emerg Infect Dis, 2007; 13(11): 1625–31.

Handayani D, Edrada RA, Proksch P, Wray V, Witte L, van Ofwegen L, Kunzmann A. New oxygenated sesquiterpenes from the Indonesian soft coral *Nephthea chabrolii*. J Nat Prod, 1997; 60(7):716–8.

Hu J, Yang B, Lin X, Zhou X, Yang X, Long L, Liu Y. Chemical and biological studies of soft corals of the *Nephtheidae* family. Chem Biodivers, 2011; 8(6):1011–32.

Huber W, Koella JC. A comparison of three methods of estimating $EC_{50}$ in studies of drug resistance of malaria parasites. Acta Trop, 1993; 55(4):257–61.

Ibezim A, Debnath B, Ntie-Kang F, Mbah CJ, Nwodo NJ. Binding of antitrypanosomal natural products from African flora against selected drug targets: a docking study. Med Chem Res, 2017a; 26(3):562–79.

Ibezim A, Nwodo NJ, Nnaji NJ, Ujam OT, Olubiyi OO, Mba CJ. In silico investigation of morpholines as a novel class of trypanosomal triosephosphate isomerase inhibitors. Med Chem Res, 2017b; 26(1):180–9.

Jackson LK, Goldsmith EJ, Phillips MA. X-ray structure determination of *Trypanosoma brucei* ornithine decarboxylase bound to D-ornithine and to G418: insights into substrate binding and ODC conformational flexibility. J Biol Chem, 2003; 278(24):22037–43.

Jacob M, Lopata AL, Dasouki M, Abdel Rahman AM. Metabolomics toward personalized medicine. Mass Spectrom Rev, 2019; 38(3):221–38.

Kapojos MM, Mangindaan REP, Nakazawa T, Oda T, Ukai K, Namikoshi MJC. Three new nardosinane type sesquiterpenes from an Indonesian soft coral *Nephthea* sp. Chem Pharm Bull, 2008; 56(3):332–4.

Kitagawa I, Cui Z, Son BW, Kobayashi M, Kyogoku YJC. Marine natural products. XVII. Nephtheoxydiol, a new cytotoxic hydroperoxy-germacrane sesquiterpene, and related sesquiterpenoids from an Okinawan soft coral of *Nephthea* sp. (*Nephtheidae*). Chem Pharm Bull, 1987; 35(1):124–35.

Kjer J, Debbab A, Aly AH, Proksch P. Methods for isolation of marine-derived endophytic fungi and their bioactive secondary products. Nat Protoc, 2010; 5(3):479–90.

Lotfy MM, Sayed AM, AboulMagd AM, Hassan HM, El Amir D, Abouzid SF, El-Gendy AO, Rateb ME, Abdelmohsen UR, Alhadrami H, Mohammed R. Metabolomic profiling, biological evaluation of *Aspergillus awamori*, the river Nile-derived fungus using epigenetic and OSMAC approaches. RSC Adv, 2021; 11(12):6709–19.

Macintyre L, Zhang T, Viegelmann C, Martinez IJ, Cheng C, Dowdells C, Abdelmohsen UR, Gernert C, Hentschel U, Edrada-Ebel R. Metabolomic tools for secondary metabolite discovery from marine microbial symbionts. Mar Drugs, 2014; 12(6):3416–48.

Mahmoud BK, Hamed ANE, Samy MN, Abdelmohsen UR, Attia EZ, Fawzy MA, Refaey RH, Salem MA, Pimentel-Elardo SM, Nodwell JR, Desoukey SY, Kamel MS. Metabolomic profiling and biological investigation of *Tabebuia Aurea* (*Silva Manso*) leaves, family *Bignoniaceae*. Nat Prod Res, 2021; 35(22):4632–7.

Molyneux DH, Savioli L, Engels D. Neglected tropical diseases: progress towards addressing the chronic pandemic. Lancet, 2017; 21(1):312–25.

Pays E. Expression and function of surface proteins in *Trypanosoma brucei*. Mol Biochem Parasitol, 1999; 91(1):3–36.

Said AAE, Afifi AH, Ali TF, Samy MN, Abdelmohsen UR, Fouad MA, Attia EZ. NS3/4A helicase inhibitory alkaloids from *Aptenia cordifolia* as HCV target. RSC Adv, 2021; 11(52):32740–9.

Scholz C, Knorr S, Hamacher K, Schmidt B. DOCKTITE-a highly versatile step-by-step workflow for covalent docking and virtual screening in the molecular operating environment. J Chem Inf Model, 2015; 55(2):398–406.

Shady NH, Elfakharany Z, Salem MA, Ahmed S, Fouad MA, Kamel MS, Krischke M, Mueller MJ, Abdelmohsen UR. Dereplication analysis and antitrypanosomal potential of the red sea sponge *Amphimedon* sp. supported by molecular modeling. Rev Bras Farmacogn, 2020; 30: 290–4.

Steverding D. The development of drugs for treatment of sleeping sickness: a historical review. Parasit Vectors, 2010; 3(1):1–9.

Su JH, Dai CF, Huang HH, Wu YC, Sung PJ, Hsu CH, Sheu JH. Terpenoid-related metabolites from a formosan soft coral *Nephthea chabrolii*. Chem Pharm Bull, 2007; 55(4):594–7.

Tawfike AF, Viegelmann C, Edrada-Ebel R. Metabolomics and dereplication strategies in natural products. Methods Mol Biol, 2013; 1055:227–44.

Ueno AK, Barcellos AF, Costa-Silva TA, Mesquita JT, Ferreira DD, Tempone AG, Romoff P, Antar GM, Lago JHG. Antitrypanosomal activity and evaluation of the mechanism of action of diterpenes from aerial parts of *Baccharis retusa* (*Asteraceae*). Fitoterapia, 2018; 125:55–8.

Yuliana ND, Khatib A, Choi YH, Verpoorte R. Metabolomics for bioactivity assessment of natural products. Phytother Res, 2011; 25(2): 157–69.

Zeouk I, Sifaoui I, López-Arencibia A, Reyes-Batlle M, Bethencourt-Estrella CJ, Bazzocchi IL, Bekhti K, Lorenzo-Morales J, Jiménez IA, Piñero JE. Sesquiterpenoids and flavonoids from *Inula viscosa* induce programmed cell death in kinetoplastids. Biomed Pharmacother, 2020; 130: 110518.

Zhang WH, Williams ID, Che CT. Chabrolols A, B and C, three new norditerpenes from the soft coral Nephthea chabroli. Tetrahedron Lett, 2001; 42(28):4681–5.

**How to cite this article:**
Allam KM, Mostafa YA, Abdelmohsen UR, Khedr AIM, Allam AE, Fouad MA, Elkhayat ES. Antitrypanosomal potential of the red sea soft coral *Nephthea mollis* supported by metabolomics profiling and molecular docking studies. J Appl Pharm Sci, 2023; 13(07):270–281.